Journal of Thermal Analysis and Calorimetry, Vol. 87 (2007) 2, 401–409

RESISTANCE OF ZINC THERMAL SPRAYED COATINGS ON DIFFERENT CORROSIVE ENVIRONMENTS

G. Vourlias, N. Pistofidis, D. Chaliambalias, K. Chrissafis[*]*, El. Pavlidou and G. Stergioudis*

Physics Department, Aristotle University of Thessaloniki, 54124 Thessaloniki, Greece

Zinc coatings on ferrous substrates are possible to be applied with thermal spraying. In the present work the corrosion behavior of zinc thermal sprayed coatings deposited on low carbon steel St-37 was examined in a simulated marine atmosphere (salt spray chamber-SSC) and in a dry atmosphere at elevated temperature (400°C). The corrosion progress was examined by means of optical microscopy, scanning electron microscopy, X-ray diffraction and thermogravimetric analysis. From this investigation it was deduced that in the SSC the coating is uniformly corroded, while the main corrosion products are hydrated zinc oxides and chlorides. By contrast at 400°C only a thin, compact and continuous film of ZnO is formed on top of the coating, which remains adherent to the ferrous substrate.

Keywords: *corrosion, SEM, TG, thermal spray, XRD, zinc coatings*

Introduction

One of the most important products of the worldwide metal production is zinc, although its usage started only about 250 years ago [1] and it is only the 23rd among the elements in relative abundance in the earth's crust [2]. The huge demand for this metal is mainly due to its application as a corrosion protective coating for ferrous materials. The position of zinc in the electromotive series of metals indicates that the coatings of this metal not only prevent contact between the underlying steel and the environment (barrier protection) but also provides a sacrificial protection due to the fact that zinc is cathodic to steel [3].

Several methods have been developed for the deposition of zinc coatings [4–6], one of which is zinc thermal spraying or metallizing [4–8]. In this case metallic zinc in the form of powder or wire is fed to a torch with which it is heated to its melting point. The resulting molten or nearly molten droplets are accelerated in a gas stream and projected against the surface to be coated (i.e., the substrate). On impact, the droplets flow into thin lamellar particles adhering to the surface, overlapping and interlocking as they solidify. The total coating thickness is usually generated in multiple passes of the coating device. Heat for melting is provided either by combustion of an oxygen-fuel gas flame or by electric arc.

In any case this method produces thick coatings composed by large sized grains. Intrinsic characteristics of these coatings are high porosity and very rough surface [9–11]. Furthermore, due to the fast cooling procedure of the liquid droplets, diffusion at the Fe–Zn interface is prohibited and as a result the coating adherence mechanism is mostly mechanical, depending on the kinetic energy of the sprayed particles, while no Fe–Zn alloy layers are present as in the case of hot-dip galvanizing [3–7].

Metallizing can be applied to ferrous materials of nearly any size. However abrasive cleaning of the steel is required prior to the coating procedure, while the high coating porosity renders sealing with a low viscosity organic liquid such as silicone or polyurethane oil necessary [8]. However these disadvantages are insignificant, because zinc metallizing is characterized by very high versatility as it does not require special installations and it is applicable also in field, by contrast to the competitive techniques which are applicable only in shop and therefore are in many cases inapplicable [4–6]. Furthermore it provides much thicker coatings suitable for heavier application such as marine. For that purpose the present work focuses on the corrosion behaviour in marine atmosphere.

Also high elevated temperature was chosen because it is frequent in unit operations which involve heat transfer with superheated steam or hot oils through steel tubes and pipes [12]. Higher temperatures are not likely because zinc melts at 419°C [13] and hence it is not possible to offer any protection above this temperature [14].

The morphology and the structure of these coatings have already been reported [4–9]. However their corrosion performance is not examined in details. Only rough descriptions are provided focusing on the empir-

* Author for correspondence: hrisafis@physics.auth.gr

1388–6150/$20.00

Akadémiai Kiadó, Budapest, Hungary
Springer, Dordrecht, The Netherlands

ical assessment of the service life of the coating in the atmosphere at ambient temperature [2]. There are no data referring to the corrosion mechanism, while the behaviour at elevated temperature is not considered at all. The thermogravimetric measurements is an ideal method for studying the corrosion behaviour of zinc thermal sprayed coatings because of its ability to simulate harsh corrosive environments [15].

In the present work an effort is made to clarify the corrosion mechanism of zinc thermal sprayed coatings under different environments (in a simulated marine atmosphere and in a dry atmosphere at elevated temperature) and to correlate the corrosion behaviour with the coating structure. Furthermore a comparison with literature data referring to hot-dip galvanized steel was also accomplished.

Experimental

Hot-rolled sheets of steel (100 mm long×30 mm wide×3 mm thick) containing 0.11% C, 0.55% Mn, 0.012% Si and 0.016% P (low carbon steel St-37) have been coated using a METCO 14E wire flame spray device. Prior to the coating deposition the surface of the ferrous substrates was sandblasted. The distance between the flame and the substrate was 120 mm, while the combustible gas was acetylene and the wire used had 2.4 mm diameter and it was composed by 99.9% pure Zn. The thickness of the as-grown coatings was about 250 μm. Part of the as-coated coupons was sealed with silicon based oil, while the rest of them were naked (unsealed).

For the examination of the corrosion in a marine atmosphere, the as-cast specimens were hanged vertically with nylon fibers at about the center of the working volume of a SC-450 Weiss Umwelttechnik Salt Spray Chamber (SSC). The uncoated sides of the coupons were covered with bee wax in order to be protected from the environment in the SSC. The corrosive medium was a 5 mass% solution of NaCl in de-ionized water. The temperature of the chamber was 40°C. Specimens were retrieved from the chamber after 48, 144, 240 and 336 h (2, 6, 10 and 14 days, respectively).

The study of the corrosion at elevated temperature was accomplished with thermogravimetric measurements (TG), which was carried out with a Setaram SETSYS TG-DTA 1750°C. The samples were placed in alumina crucibles. An empty alumina crucible was used as reference. During non-isothermal experiments the samples were heated from ambient temperature to 450°C in a 50 mL min^{-1} flow of air with heating rate of 10°C min^{-1} and continuous records of sample temperature, sample mass, its first derivative and heat flow were taken. For the isothermal experiments the samples at first were heated from ambient temperature to 400°C in a 50 mL min^{-1} flow of air with heating rate of 10°C min^{-1} and then they remained for 24 h at this temperature.

In every case, for the study of corrosion progress the surface of the corroded specimens was examined with a Karl Zeiss M8 low magnification binocular light microscope equipped with a CCD camera for image capture. Afterwards cross sections have been cut from each sample, mounted in bakelite and polished down to 5 μm alumina emulsion. The as-prepared coupons were observed with an Olympus BX60 light microscope connected with a digital camera CCD JVC TK-C1381.

The nature of the phases formed was determined with X-ray diffraction (XRD) and scanning electron microscopy (SEM) associated with an EDS analyser. For the XRD experiments a 2-cycles Seifert 3003 TT diffractometer (CuK_α radiation) with Bragg–Brentano geometry was used, while the SEM study was accomplished with a 20 kVolt JEOL 840A SEM equipped with an Oxford ISIS 300 EDS analyzer and the necessary software for point microanalysis, linear microanalysis and chemical mapping of the surface under examination. The coated surface of the samples was observed with SEM without any preparation, while for the examination of the cross-section the surface of the samples was polished in a similar way with the preparation for optical microscopy.

Results and discussion

Corrosion in a simulated marine atmosphere

The mechanism of the atmospheric corrosion of zinc has been thoroughly studied [2, 16–20]. In a non-polluted moist atmosphere zinc is initially covered by a thin layer mainly composed by zinc hydroxide. After a short exposure period (ranging from a few weeks to a few months) zinc hydroxide dehydrates to form zinc oxide or reacts with the carbon dioxide dissolved in water to form zinc carbonate or basic zinc carbonate. The formation of this film slows down the corrosion rate.

However this process is disturbed when considerable amounts of pollutants, such as Cl^- ions, are present in the air, which destabilize the carbonate film and thus accelerate corrosion. Under these conditions the predominant mechanism is uniform corrosion although the formation of pits along the coating surface (pitting corrosion) is also possible [2, 21, 22]. Moreover a mechanism of intergranular corrosion is probable, although it is not usual. In this case irregularities of the crystal structure of the coating, such as the precipitation of phases at the grain boundaries, trigger this mechanism and as a result the corrosive ionic species attack preferentially the grain boundaries with relatively little corrosion of the grains [2]. Finally entire

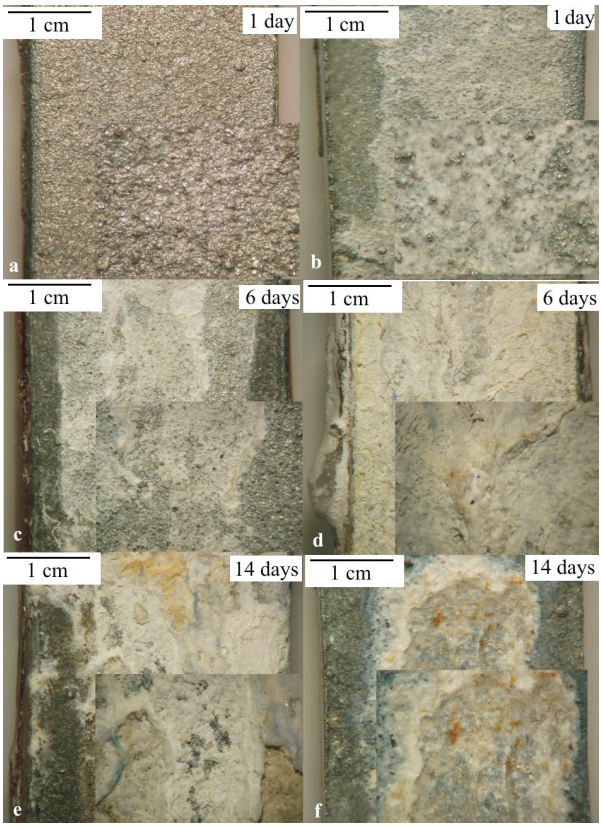

Fig. 1 Stereoscopic photographs of the corroded samples; a, c and e – refer to sealed coatings, while b, d and f – refer to unsealed coatings. The inset photographs present the same area at higher magnification

grains are detached from the coating because their boundaries are decomposed.

In the present work the thermal sprayed coatings on the particular steel substrate were exposed in a simulated marine atmosphere, where a high Cl^- content is present. To clarify their corrosion mechanism the corroded samples were initially examined with a low magnification binocular light microscope (Fig. 1). From the examination of the photographs of Fig. 1 it is obvious that the exposure of the coated coupons in the SSC resulted at the formation of voluminous corrosion products. It could be also deduced that the coating degradation began very early. In the case of unsealed coupons it started from the first day of exposure (Fig. 1b). The sealer application delayed this phenomenon by about one day (Fig. 1a). Only after the second day of exposure the layer of the corrosion products was visible with naked eye. Probably by that time the organic layer was washed off by the continuous flow of the corrosive medium and the underlying zinc was exposed.

The same conclusions could be drawn from the SEM observation of the coating surface (Fig. 2). After 48 h (2 days) of exposure (Fig. 2a) only a rather thin film of corrosion products was observed on the sealed coatings. The morphology of the underlying

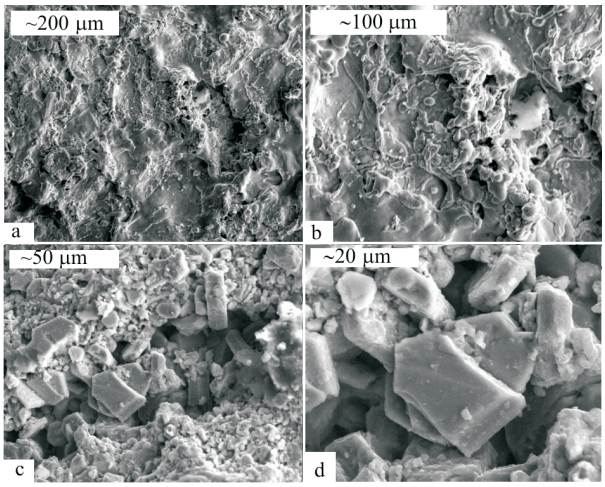

Fig. 2 SEM micrographs of the corroded coatings; a, b – after 2 days of exposure, c, d – after 6 days of exposure

zinc surface is still clearly distinguished. However the EDS analysis reveals high oxygen concentration along with chlorine, which means that corrosion had began already, although the results were not severe.

The EDS analysis of the corroded samples retrieved after 144 h (6 days) showed that the corrosion products are composed by zinc (Zn), oxygen (O) and chlorine (Cl) at different concentrations. Consequently, zinc oxides and chlorides had been already formed by that time. Zinc hydroxyl compounds were also expected, but hydrogen detection is not possible with EDS. Nevertheless some crystals of NaCl were also detected originating to the crystallization of the corrosive medium. The SEM micrographs of the same coupons (Fig. 2b) showed that the coating surface is totally covered by the corrosion products. However, no red rust (iron oxides) appeared on the surface of the samples until the 14^{th} day of exposure (Figs 1e and f). Even by that time their formation was only localized and not generalized. Hence it could be attributed to coating failure in some areas where probably defects were already present from the deposition process.

What is characteristic in the examined samples is the fact that the color of the corrosion products remained white up to the 14^{th} day of exposure. By contrast, in the case of hot-dip galvanized coatings the initial white coloration soon changes into grayish because of the formation of iron oxides due to the iron content of the coating. This phenomenon is not observed in this case because the coating does not contain any iron [22].

The composition of the corrosion products was detected more precisely with XRD (Fig. 3). The presented XRD patterns refer to sealed samples after 6 (Fig. 3a) and 14 days of exposure (Fig. 3b). In both cases the predominant compounds are hydrated Zn oxides and chlorides. Reflections referring to Fe compounds were not recorded even after 14 days of

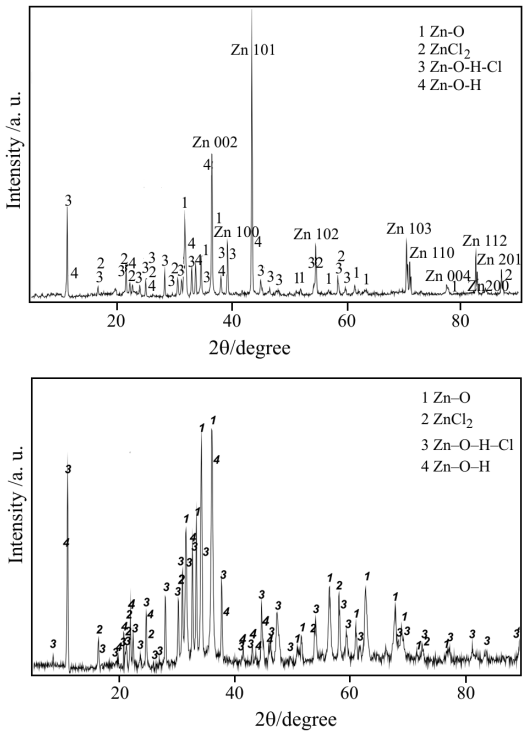

Fig. 3 XRD patterns of sealed coatings after a – 6 and b – 14 days of exposure [23]

exposure, probably due to the low content of these compounds and the high coating thickness which did not allowed the X-ray beam to penetrate up to the ferrous substrate. It is also obvious that the quantity of the corrosion products increased with regard to the exposure time, as the increase of the intensity of the peaks shows. In any case the XRD patterns verify the EDS observations.

For a better understanding of the corrosion progress, the cross-section of the samples was examined with optical microscopy (Fig. 4). From these micrographs it is obvious that the corrosion of both types of coatings (sealed and unsealed) is uniform. In the case of unsealed specimens after six days of exposure large cavities are observed (Fig. 4c), which are likely to be smaller for the sealed coatings. Neither pitting nor intergranular corrosion was observed. After 14 days of exposure total failure of both coatings is locally observed. At these points the surface of the ferrous substrate is exposed (Figs 4e and f). These areas probably lead to the formation of red rust stains which were observed with the stereoscope.

The SEM micrographs of the coating cross-section along with the chemical mapping of the examined surface (Figs 5 and 6) offer more information. Uniform corrosion is observed also with this method, while no

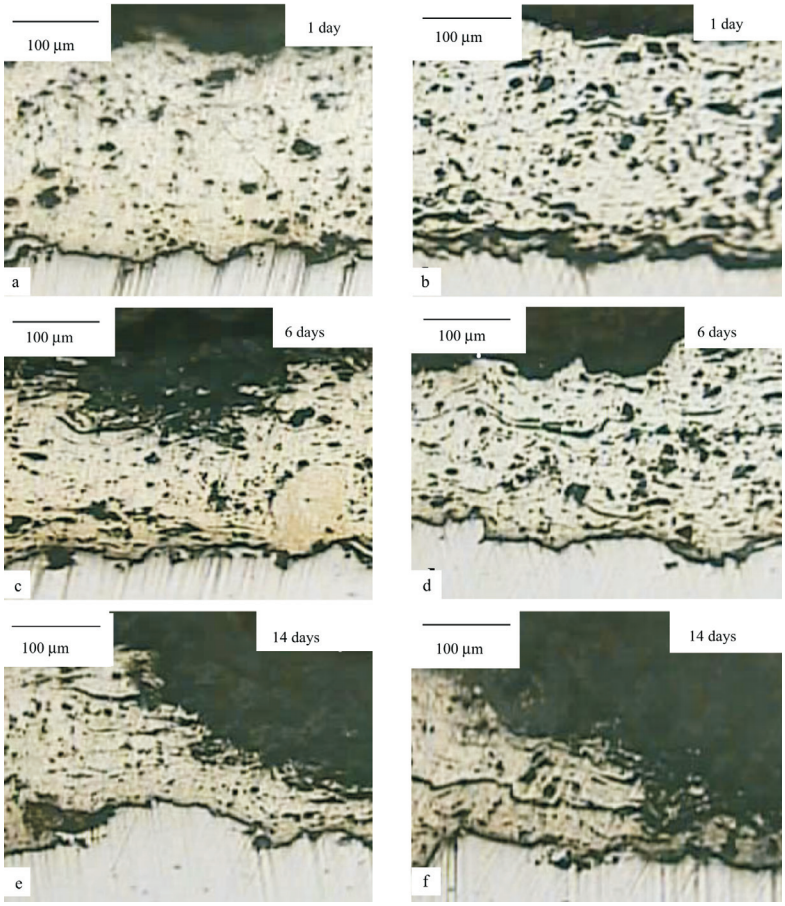

Fig. 4 Optical micrographs of the a, c, e – unsealed and b, d, f – sealed coatings

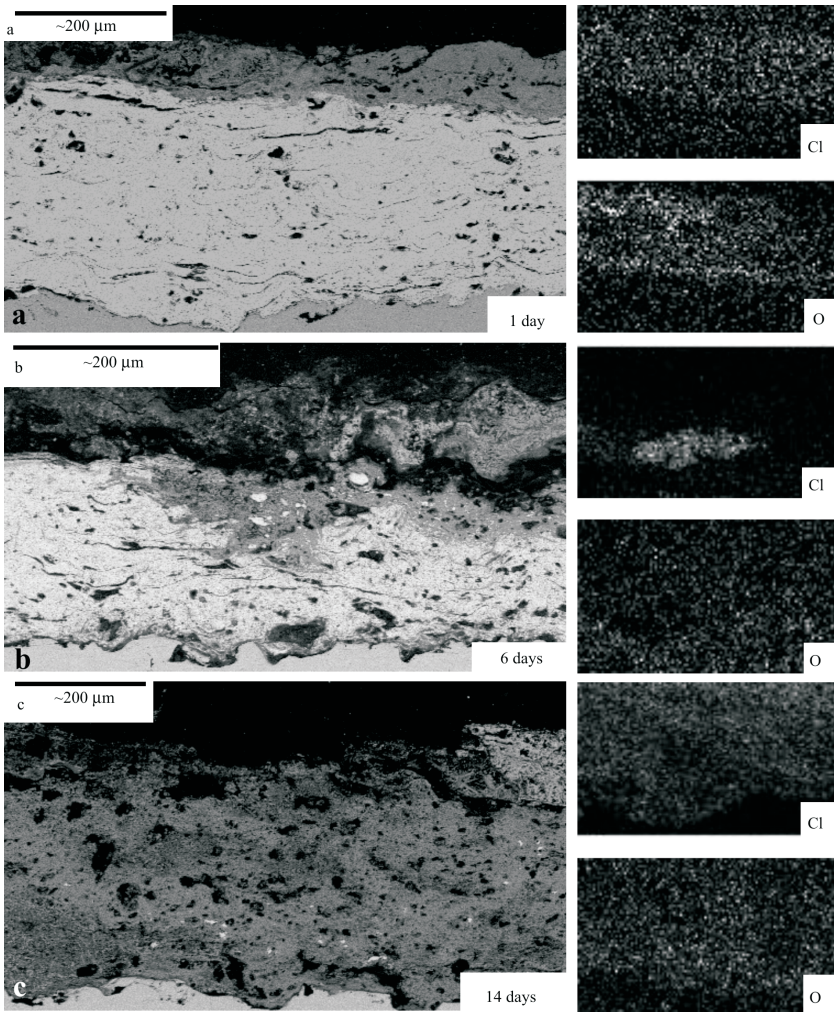

Fig. 5 SEM micrographs of the unsealed coatings. The chemical mappings present chlorine and oxygen distribution after 1, 6 and 14 days of exposure

preferred nucleation sites for corrosion were observed. Furthermore the penetration of every corrosive element in the coating is clearly indicated by the different hue of the coating in each micrograph (where darker areas refer to affected parts of the coating), while the results of chemical mapping are even more enlightening on this subject.

The initial attack takes place at the coating surface (Figs 5a and 6b). Chlorine and oxygen react with zinc (without excluding hydrogen from water droplets, which unfortunately is not possible to be detected due to the inherent limitations of SEM). As the superior zinc layer is destabilized these reactions continue deeper in the coating. As a result they gradually lead to its decomposition (Figs 5c and 6c). These phenomena are similar regardless the application of sealer, which only delays their progress without interfering to the corrosion mechanism. Furthermore they do not seem to be affected by the coating porosity.

From the above examination it could be concluded that the only corrosion mechanism of the zinc thermal sprayed coatings on the particular steel substrate exposed in a SSC was uniform corrosion, a phenomenon which was not reported with the other zinc coatings [2, 17–22]. Pitting and intergranular corrosion were not observed. The absence of the intergranular corrosion could be easily justified by taking into account the fact that the coating composition and crystal structure is homogeneous. Hence there are not any different phases at the grain boundaries that could facilitate diffusion.

The absence of pitting corrosion is not so plausible. The localized attack and the formation of pits on the coating surface are usually attributed to a local breakdown of the carbonate film covering the zinc coating, as chloride ions are specifically absorbed on certain sites of the carbonate film [2, 22]. As these ions penetrate into the film, they lead to its breakdown, following a complicated electrochemical mechanism involving the local acidification of the solution trapped in the pits [2]. Consequently the extent of pitting corrosion is determined by the existence of nucleation sites

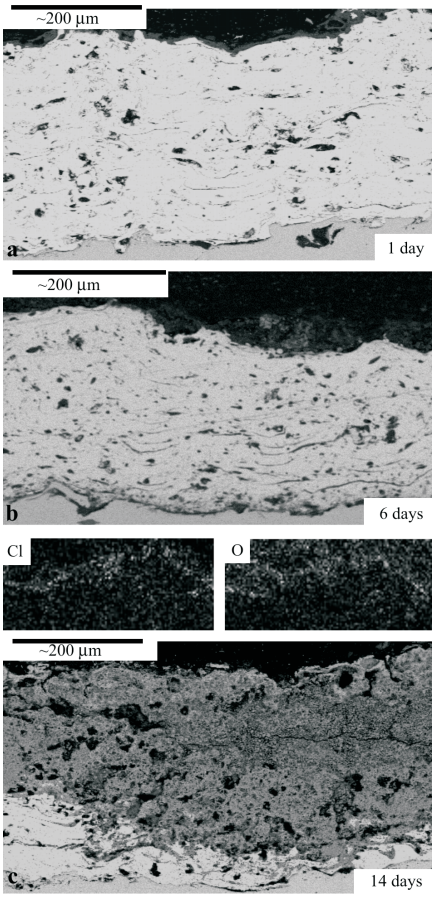

Fig. 6 SEM micrographs of the sealed coatings. The chemical mappings present chlorine and oxygen distribution after 6 days of exposure

on the carbonate film where Cl^- ions could be absorbed. Absorption at these sites is facilitated by local defects of the crystalline structure of the film, such as the presence of impurities on the coating surface (dross or ash from the galvanizing kettle [24]) or the low thickness of the carbonate film. The later is likely to be favoured by the existence of rough surfaces that impede the transport of the necessary species and delay the film growth. In the case of thermal sprayed coatings the surface is extremely rough. Hence the carbonate film thickness is expected to be lower than in other zinc coatings. As a result it is highly possible that the whole film is weakened through the effect of the Cl^- ions and its breakdown occurs over the whole surface, leading only to uniform corrosion.

Thus, although thermal sprayed coatings are composed by only pure zinc and their corrosion behaviour would be expected to be similar to that of zinc as it is reported in the literature [2], differences were recorded. A possible reason, as it was mentioned earlier, is the fact that thermal sprayed coatings are characterized by high surface roughness which affects the corrosion mechanism. The high coating porosity would be also expected to affect corrosion resistance, because the existence of pores usually facilitates diffusion of the corrosive species. However in the thermal sprayed coatings the pores do not communicate and do not form a network. As a result they are rather inert.

As far as it concerns the estimated service life of the coatings in a marine atmosphere, it was not possible to establish any model predicting corrosion rate due to the lack of field exposure data, since a simulated environment is used. However a comparison with the performance of zinc hot-dip galvanized coatings would be feasible, because these coatings are already examined under the same circumstances [22]. Furthermore, a comparison of this kind would be also very useful because hot-dip galvanized coatings represent the most widely produced category of industrial zinc coatings [3] and therefore they are usually considered as a reference point.

Anyway, it seems that the coatings under examination are as resistant as the hot-dip galvanized coatings, if we take into account the necessary time for the appearance of red rust in the SSC [22]. However, hot-dip galvanized coatings are usually much thinner (50–80 μm). Thus, in fact the thermal sprayed coatings are less resistant. A probable reason for this difference is the absence of the Fe–Zn phases, which are more resistant than pure zinc [2, 3]. As a result when the outer layer of the hot-dip galvanized coatings is consumed, the exposed phases offer better protection and corrosion progress is slowed down. A similar phenomenon is not observed in the thermal sprayed coatings due to the lack of the Fe–Zn phases.

Corrosion at elevated temperature

The elevated temperature was verified with the help of non-isothermal measurements of the mass change of the samples. In Fig. 7 the simultaneous mass increase along with the heat flow are presented. As it can be seen in these plots the mass of the samples starts to increase above 380°C. The endothermic peak at the heat flow curve corresponds to the melting of Zn (419°C). Above 419°C the rate of the mass change increases due to the zinc melting. This could be attributed to the fact that zinc liquefaction leads to stripping of the underlying steel. As a result the substrate is not protected anymore. These observations verify that, at the chosen temperature (400°C), oxidation is possible to be studied with satisfactory results, because a certain progress will be recorded with a safe distance from zinc melting which could provoke total collapsing of the system due to zinc melting.

In Fig. 8 the mass increase *vs*. time is presented for a zinc thermal sprayed coating at 400°C after 24 h of exposure. As it can be seen in this plot the oxidation rate is initially very high and gradually dimin-

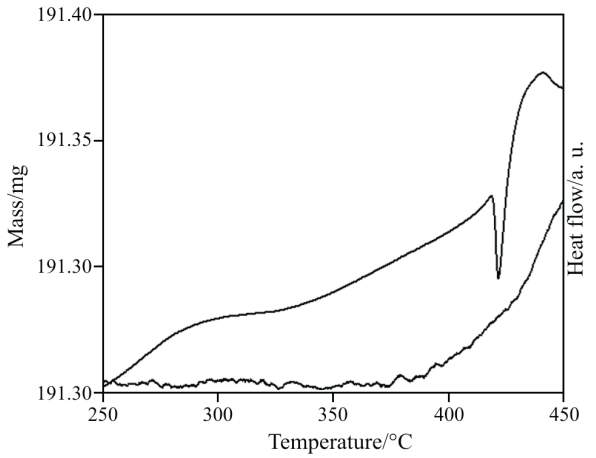

Fig. 7 Increase of mass and heat flow change *vs*. temperature

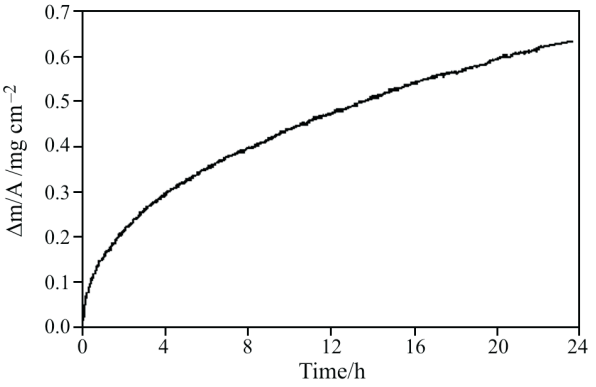

Fig. 8 Increase of mass *vs*. time at 400°C

ishes. However even after 24 h of exposure, although it is rather low there is not any plateau in the diagram and hence the corrosion is not nullified.

Afterwards, the cross-section and the plain view of the as-oxidized coatings were examined with SEM. A thin, compact and continuous film was observed without any cracks and with an average thickness of less than 5 μm, which seems to totally cover the underlying zinc in the form of a sheet (Figs 9 and 10). Its EDS analysis showed that it was composed by zinc and oxygen while no other element, such as chlorine, was detected. The ZnO film is already present prior to the exposure of the specimens at 400°C [22]. Hence this film is initially formed in ambient temperature. As the temperature rises, it is further grown due to the progress of the reaction of zinc and oxygen with regard to the exposure time.

At the temperature under examination (400°C) the corrosion mechanism of metallic materials is different from the mechanism in a simulated marine atmosphere. Electrochemical corrosion (in the conventional meaning of the expression – as it was previously described) does not take place. In this case a different mechanism is considered which in fact is also electro-

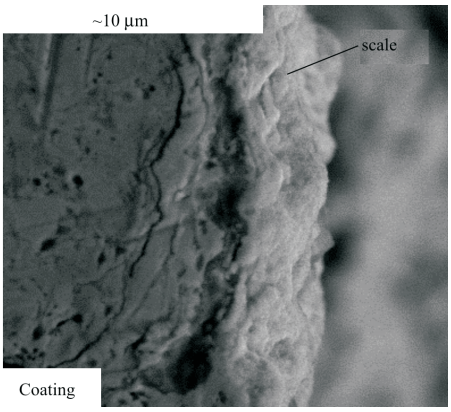

Fig. 9 SEM micrograph of the cross-section of the ZnO scale formed on the thermal coating after 24 h of exposure at 400°C

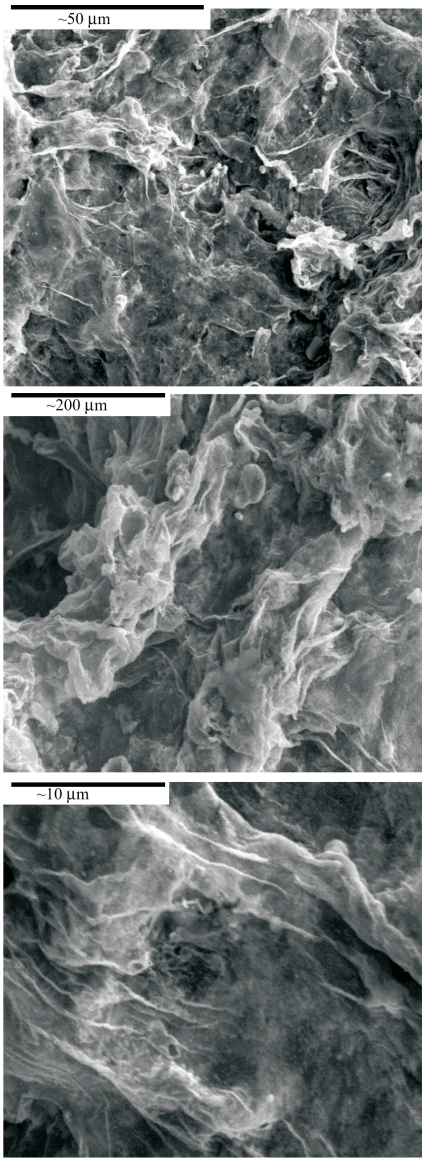

Fig. 10 SEM micrographs of the plane view of the ZnO scale formed on the thermal coating after 24 h of exposure at 400°C. The same area is presented at every micrograph at different magnification

chemical but without the interference of an aqueous phase [14, 25, 26]. This mechanism postulates that a metal oxide film (scale) is already formed on the coating surface when the coating is exposed to the corrosive environment, which is the case for zinc. In this environment oxygen from the gaseous phase is reduced to oxygen ions at the scale-gas interface, while metal ions are formed at the metal-scale interface. The produced electrons from the oxidation reaction diffuse through the already formed oxide layer, along with metal cations and oxygen anions, which are combined to form new metal oxide lattice sites. With regard to the conductivity of the two ionic species (metal cations and oxygen anions), the growth of the metal oxide layer could be at the metal-scale interface or at the scale-gas interface.

The ZnO layer behaves as an n-type semiconductor [2] and thus its typical electronic conductivity ($1\ \Omega^{-1}\ cm^{-1}$ [2]) is adequate to ensure the progress of the oxidation reactions. However there are not enough experimental data collected in the present work to establish whether the coating growth takes place at the scale-gas or at the metal-scale interface, i.e. if the metal cation or the oxygen anion diffusion controls the progress of the procedure.

In the oxide-scale formation on pure metals generally all the potential stable oxide phases are formed [14, 25]. However in this case the EDS analysis of the cross-section of the ZnO scale indicates that it is rather homogeneous from a compositional point of view. This phenomenon could be attributed to the fact that from only ZnO is stable at 400°C [13].

In any case the low thickness of the scale indicates that its growth rate is rather low. Nevertheless its continuity and uniformity imply that it is protective, because, if we take into account the fact that ionic diffusion controls the kinetics of the process, it is expected that after a certain period of time the increase of the coating thickness would impede ionic diffusion and thus its growth would be practically interrupted. This conclusion is also supported by the TG plot of Fig. 8, where a decrease of the rate of the mass change is recorded with regard to the exposure time.

Another important observation is related to the fact that the coating remained adherent to the ferrous substrate at 400°C (Fig. 11). Under the same conditions hot-dip galvanized coatings are characterized by total failure due to peeling [27]. As far as it concerns zinc thermal sprayed coatings the superior mechanical behavior could be attributed to the high zinc ductility and low hardness [28]. Zinc and iron are characterized by a very intense mismatch of their thermal expansion coefficients [28]. Due to this fact tensile internal stresses are induced in the Fe–Zn phases of the hot-dip galvanized coatings during their cooling after their removal from the liquid zinc [28]. These stresses are relieved through the formation of cracks in the coating perpendicular to the ferrous substrate.

Fig. 11 Stereoscopic photographs of the surface of zinc thermal sprayed coatings after 24 h of exposure at 400°C

The mismatch of the thermal expansion coefficients affects also the coating performance at elevated temperatures, when both the substrate and the coating expand. Since dimensional change of the substrate is not in accordance with that of the coating, compressive stresses are induced in the later. In the case of hot-dip galvanized coatings the high hardness and low ductility of Fe–Zn phases [28] result to peeling. However in the zinc thermal sprayed coatings the Fe–Zn phases are absent. The high ductility and low hardness of zinc result to a relief of the induced stresses through plastic deformation of the coating. This assumption could be also supported by the ridges of the scale which are observed in Fig. 10 and could be caused by a deformation of the underlying phase.

To sum up, from the above examination it could be deduced that thermal sprayed coatings are more resistant at elevated temperature with regard to the hot-dip galvanized. However, their superior performance is only affected by their superior mechanical behavior.

Conclusions

Concerning the corrosion resistance of zinc thermal sprayed coatings in a salt spray chamber it was deduced that the predominant corrosion mechanism is uniform degradation. Other corrosion forms encountered with zinc were not observed. Furthermore the main corrosion products are hydrated zinc oxides and chlorides. Fe oxides were also observed. Moreover corrosion performance is not affected by the porosity, while the surface roughness seems to favor uniform corrosion. In any case hot-dip galvanized coatings are more resistant under the same circumstances due to the presence of Fe–Zn phases.

Concerning the durability of zinc thermal sprayed coatings at 400°C it was deduced that a thin, compact and continuous film of ZnO is formed on top

of the coating, which is probably protective. Nevertheless, the coating remained adherent to the substrate at 400°C, due to its high ductility and low hardness. By contrast the hot-dip galvanized coatings tend to peel under the same conditions.

References

1 F. Habashi, Discovering the 8th metal-A history of zinc, IZA.
2 X. G. Zhang, Corrosion and Electrochemistry of Zinc, Plenum Press, New York 1996.
3 A. R. Marder, Prog. Mater. Sci., 45 (2000) 191.
4 N. Pistofidis, G. Vourlias, D. Chaliampalias, E. Pavlidou, K. Chrissafis, G. Stergioudis, E. K. Polychroniadis and D. Tsipas, J. Therm. Anal. Cal., 84 (2006) 191.
5 N. Pistofidis, G. Vourlias, E. Pavlidou, K. Chrissafis, G. Stergioudis, E. K. Polychroniadis and D. Tsipas, J. Therm. Anal. Cal., 86 (2006) 417.
6 Zinc coatings, American Galvanizing Association, Englewood, Colorado 2000.
7 R. C. Tucker, Thermal Spray Coatings, in Vol. 5, Surface Engineering, American Society of Metals, ASM International, 1996.
8 Engineering and Design-Thermal Spraying: New Construction and Maintenance, CECW-ET, Engineer Manual 1110-2-3401, Department of the Army, U.S. Army Corps of Engineers, Washington 1999.
9 D. Chaliampalias, G. Vourlias, N. Pistofidis, I. Tsiaoussis, E. Pavlidou and E. K. Polychroniadis, on the Effect of Nanocrystalline ZnO Particles on the Anticorrosive Behaviour of Flame Sprayed Zinc Coatings, IMC 2006, Sapporo, Japan.
10 G. Vourlias, N. Pistofidis, G. Stergioudis and E. K. Polychroniadis, J. Alloys Compd., 416 (2006) 183.
11 G. Vourlias, N. Pistofidis, P. Patsalas, E. Pavlidou, G. Stergioudis and E. K. Polychroniadis, High Temp. Mater. Processes, 9 (2005) 243.
12 M. J. Mitchell, Developments in Coatings for High Temperature Corrosion Protection, Proceedings of the SSPC 2002 Technical Presentations, Tampa, Florida, November 3–6, 2002, pp. 88–96.
13 D. R. Lide (Ed.), CRC Handbook of Chemistry and Physics, 80th Ed., CRC Press, London 1999–2000.
14 M. Fontana, Corrosion Engineering, McGraw-Hill, 3rd Ed., New York 1986.
15 Dun Chen, J. Therm. Anal. Cal., 85 (2006) 13.
16 S. G. Lee and S. G. Kang, J. Mater. Sci. Lett., 16 (1997) 902.
17 S. Oesch, M. Faller, Corr. Sci., 39 (1997) 1505.
18 V. Ligier, M. Wery, J. Y. Hihn, J. Faucheu and M. Tachez, Corros. Sci., 41 (1999) 1139.
19 A. R. Mendoza and F. Corvo, Corros. Sci., 42 (2000) 1123.
20 E. Almeida, M. Morcillo and B. Rosales, Br. Corros. J., 35 (2000) 284.
21 E. Almeida, M. Morcillo and B. Rosales, Br. Corros. J., 35 (2000) 289.
22 G. Vourlias, N. Pistofidis, D. Chaliampalias, E. Pavlidou, P. Patsalas, G. Stergioudis, D. Tsipas and E. K. Polychroniadis, Surf. Coat. Technol., 200 (2006) 6594.
23 PC Powder Diffraction Files, JCPDS-ICDD, 2000.
24 G. Vourlias, N. Pistofidis, G. Stergioudis and E. K. Polychroniadis, Sol. St. Sci., 7 (2005) 465.
25 E. Mattson, Basic Corrosion Technology for Scientists and Engineers, IOM Communications, 2nd Ed., London 1996.
26 T. Brylewski, J. Dabek and K. Przybylski, J. Therm. Anal. Cal., 77 (2004) 207.
27 Hot dip galvanizing for corrosion protection of steel products, American Galvanizers Association, Englewood, Colorado 2000.
28 G. Reumont, J. B. Vogt, A. Iost and J. Foct, Surf. Coat. Technol., 139 (2001) 265.

Received: July 7, 2006
Accepted: October 10, 2006
OnlineFirst: December 18, 2006

DOI: 10.1007/s10973-006-7798-5